

# Synthesis and structural properties characterization of ha/alumina and ha/mgo nanocomposite for biomedical applications

## Abstract

HA/Alumina and HA/MgO nanocomposites were successfully prepared by using the hydrothermal method for the first time at 250°C. The mechanisms of composite formation, crystallite size, crystallinity, morphology, were studied HA/Alumina and HA/MgO nanocomposites. XRD and FTIR investigations showed an intermolecular interaction between HA/Alumina and HA/MgO. The formation of HA/Alumina and HA/MgO nanocomposites are polycrystalline in nature. It confirmed in TEM analysis. TEM images further ascertained that HA<sub>p</sub>/Alumina was formed in a short nanorod shape and HA/MgO nanocomposites show nanocluster like morphology. The FTIR measurement shows the appropriate vibrational spectra of HA/Alumina and HA/MgO nanocomposites. The UV–VIS measurements show the band–gap of HA/Alumina and HA/MgO nanocomposites. This study provides a platform for further research on the HA/Alumina and HA/MgO nanocomposites for biomedical applications.

**Keywords:** hydrothermal method, nanocomposites, hydroxyapatite, alumina, mgo, tem, x–ray diffraction

Volume 1 Issue 4 - 2017

Vijayalakshmi V

Department of Physics, Erode Sengunthar Engineering College, India

**Correspondence:** Vijayalakshmi V, Crystal Growth Laboratory, Department of Physics, Erode Sengunthar Engineering College, Erode– 638057, India, Email vijiphysics007@gmail.com

**Received:** November 18, 2017 | **Published:** December 07, 2017

## Introduction

HA– Alumina nanocomposite is biocompatible and has desirable mechanical and physical properties. Less cost, simple synthesis method, and fast production are the added advantages of this nanocomposite. Thus HA coatings on the surface of alumina substrates are used to combine excellent bioactivity of HA with superior mechanical properties of the alumina substrates. One of the elements associated with biological apatite is magnesium.<sup>1</sup> Mg incorporation into HA<sub>p</sub> stimulates osteoblast proliferation. Mg acts similar to a growth factor during the early stages of osteogenesis and promotes bone formation. Typical concentrations of carbonate and Mg ions in human bone are 5.8 and 0.55wt%, respectively. Although the extent of these elemental substitutions is minimal, they are important for biological activity and interaction between bone mineral and calcium–phosphate–based implant materials by influencing crystal growth, dissolution rate, solubility, surface chemistry and charge, morphology, and the mechanical properties. By substitution of a smaller Mg ion or Al ion for a larger Ca ion, additional structural changes may be required to prevent destabilization/decomposition of the structure during heat treatment process. This can be achieved by co–substitution of a second ion, to the HA structure.<sup>2</sup> Thus, MgO and Alumina nanoparticles dispersed within polymer composites have the potential to enhance bone tissue formation with limited adverse degradation reactions. Taking advantage of these prior studies, the objective of the present *in vitro* study was to characterize MgO and Alumina nanoparticles as additive materials for orthopedic tissue engineering applications, especially when used in combination with HA nanoparticles.<sup>3</sup>

## Materials

HA/Alumina and HA<sub>p</sub>/MgO nanocomposites were prepared using novel environmentally benign technology called hydrothermal

method. The following precursors were used for the preparation of nanocomposite. Calcium Nitrate (Ca(NO<sub>3</sub>)<sub>2</sub>·4H<sub>2</sub>O, Merck GR, 99%) is taken as the Calcium precursor. Diammonium Hydrogen Phosphate (NH<sub>4</sub>HPO<sub>4</sub>, Merck GR, 99%) is taken as the Phosphate precursor. Aluminium Nitrate (Al(NO<sub>3</sub>)<sub>3</sub>·9H<sub>2</sub>O, Merck GR, 99%) is taken as the Alumina precursor. Ammonia is taken as the pH reagent. Double distilled water is used to obtain homogeneous solution. Magnesium Nitrate hexahydrate (Mg(NO<sub>3</sub>)<sub>2</sub>·9H<sub>2</sub>O, Merck GR, 99%) is taken as the Magnesium precursor. NaOH (Merck, purity 99%) is taken as the pH reagent. Double distilled water is used to obtain homogeneous solution.

## Synthesis of nano Ha/alumina and Ha/Mgo composite

The 0.05M of Al<sub>2</sub>O<sub>3</sub> was prepared by adding 4.68g of Aluminium Nitrate dissolved in 250ml de–ionized water. Then the ammonia solution (25% of ammonia) was added to increase the pH value to 11. Thereafter the prepared solution was allowed for overnight stirring and kept undisturbed for aging. In order to synthesize nano–hydroxyapatite 5.9g of Calcium Nitrate and 1.98g of Diammonium Hydrogen Phosphate were taken in the hydrothermal vessel and mixed with de–ionized water with the molar ratio of 1:0.6 to maintain the Ca/P ratio 1.67 which is the stoichiometric ratio of HA. The pH of the above solution is increased to 9 by adding ammonia solution (25% of ammonia). The prepared Alumina solution was added drop by drop to the above solution. The vessel is placed in the oven of the hydrothermal instrument. The mixed solution was hydrothermally treated at 250°C for 5 hours. After 5 hours the autoclave is cooled to room temperature. Hydroxyapatite–Alumina nanocomposite is separated by filtration, washed a few times and kept in hot air oven at 60°C. The dried composite is ground using mortar and pestle. Similarly, the 0.1M of Mg (OH)<sub>2</sub> was prepared by adding 6.41g of Magnesium Nitrate dissolved in 100ml de–ionized water. Then the 0.8g of NaOH solution was prepared in 50 ml de–ionized water.

The NaOH solution added to increase the pH value to 11. Thereafter the prepared solution was allowed for overnight stirring and kept undisturbed for aging. Then the experimental procedure is same for HA/MgO nanocomposite was prepared at 250°C.

## Results and discussion

### XRD analysis

The X-ray diffraction patterns of the powdered nanoparticles were recorded using XRD-1008 with Cu-K $\alpha$  radiation (1.54060Å). XRD pattern for HA/Alumina and HA/MgO Nanocomposite synthesised at 250°C shows clear reflections from the (1 1 2), (0 0 2), (2 1 3) and (1 1 2), (0 0 2) (2 1 1), (3 1 0) planes in the range 25°–50°. The prepared samples show well-defined peaks which indicate high crystalline nature. All the diffraction peaks could be readily indexed with pure hexagonal phase (space group: P $_6$ /m (176)) with lattice parameters of a=9.460Å and c=6.880Å which are in accordance with the JCPDS file card number #821943. The average crystallite size of HA/MgO and HA/Alumina samples synthesised as calculated by Scherrer's formula ( $D=k\lambda/\beta\cos\theta$ ) was 8.80nm and 11.95nm respectively. The value of lattice constants obtained are a=9.4740Å, c=6.8982Å and a=7.36779Å, c=3.6837Å. The unit cell volume (V) inferred is 1602.994Å $^3$  and 1463.947Å $^3$ . 0.0103 And 0.0085 are the degree of crystallinity ( $\times_c$  (%)). The (0 0 2) peak was chosen to calculate the average crystallite size, lattice parameters, unit cell volume and degree of crystallinity for HA. It is known that the preferential growth of apatite crystal is along the c-axis.<sup>4-7</sup>

The relationship between lattice constant (a & c), Miller's indices (h,k,l) and lattice spacing (d) is used to calculate lattice parameter values, expressed as,

$$\frac{1}{d^2} = \frac{4}{3} \left( \frac{h^2 + k^2}{a^2} \right) + \frac{l^2}{c^2}$$

The volume (V) of the hexagonal unit cell and the degree of crystallinity ( $\times_c$ ) of the pure n-HA and different n-HA/SA composites are obtained using the equation, respectively,  $V=2.589 a^2 c$  and

$$\times_c = \left( \frac{K_A}{\beta} \right)^3$$

Where  $\beta$  is the full-width at half maximum,  $\times_2$  the degree of crystallinity,  $\hat{E}_A$  the constant (0.24) and a and c are lattice parameters (Figure 1A & 1B).<sup>8</sup>

### FTIR analysis

The characteristic peaks of HA/Alumina and HA/MgO nanocomposites were examined by Fourier Transform Infrared Spectroscopy (FTIR). The pellet for FTIR measurements was prepared by mixing the sample (2mg) with 200mg of IR grade KBr. The mixed powder was pressed in a stainless steel pellet die for one minute at constant pressure to obtain a translucent disc. The absorption spectra were measured at 4000–400cm $^{-1}$  using SHIMADZU spectrometer, Japan.

Biological HA is usually Calcium deficient, it is always substituted

with a carbonate. The most characteristic peaks in the FTIR spectra of synthesized HA/Alumina and HA/MgO nanocomposites are PO $_4^{3-}$ , OH $^-$ , CO $_3^{2-}$  and Al $^{3+}$ , Mg $^{2+}$ , CO $_3^{2-}$  forms a strong peak at 1381.03cm $^{-1}$  and 1396.43cm $^{-1}$ . The broad peaks appeared at 1033.85cm $^{-1}$  and 1018.41, 1072.42cm $^{-1}$  and 1080.41; indicate the presence of to the asymmetric stretching ( $\nu_3$ ) mode of vibrations because of the phosphate bonds.<sup>6,9</sup> Weak peaks in the range 560–740cm $^{-1}$  and 555–610cm $^{-1}$ , are observed due to the presence of Al $^{3+}$  ions and Mg $^{2+}$  ions.<sup>6</sup> The broad peak spread over the range between 3387–3435cm $^{-1}$  and 1635cm $^{-1}$  for HA/Alumina and 3109–3179cm $^{-1}$  and 1635.64 for HA/MgO reveals the superposition of absorption because of the stretching mode of surface hydroxyl groups and adsorbed water molecules.<sup>10</sup> OH $^-$  group forms strong and broad peaks in the range 3200–3600cm $^{-1}$  (Figure 2A & 2B) (Table 1).<sup>11,12</sup>

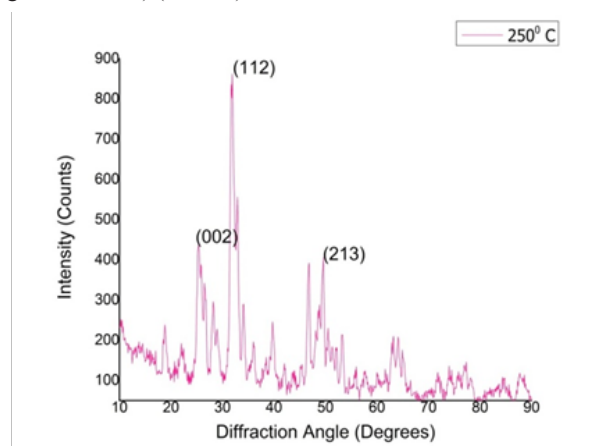


Figure 1A XRD pattern of HA/Alumina nanocomposite at 250°C.

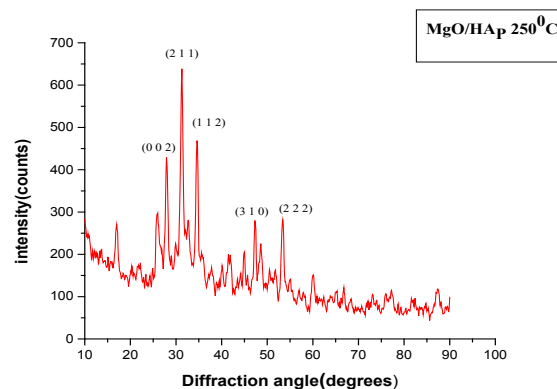


Figure 1B XRD pattern of HA/MgO nanocomposite at 250°C.

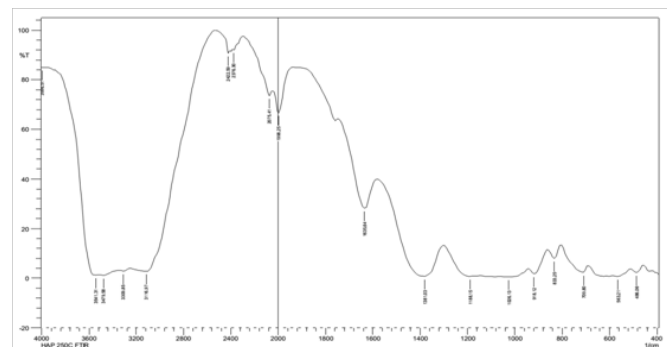


Figure 2A The FTIR spectra for HA/Alumina nanocomposite at 250°C.

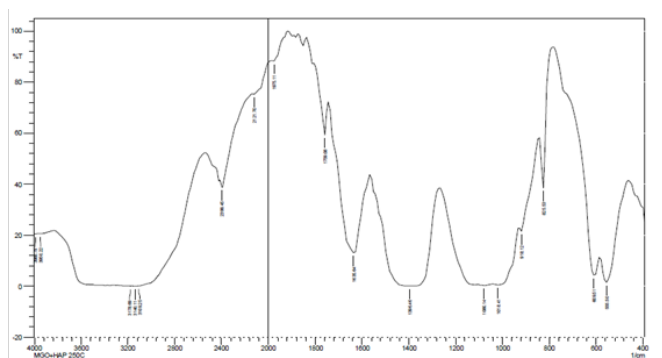


Figure 2B The FTIR spectra for HA/MgO nanocomposite at 250°C.

Table I Vibrational frequency

Vibrational frequency (Cm <sup>-1</sup> )	Assignments
<b>HA/Alumina</b>	
1381.03	Carbonate band
1033.85, 1072.42	v <sub>3</sub> asymmetric stretching of phosphate
560–740	Aluminium bands
3200–3600	Stretching mode of surface hydroxyl Groups and adsorbed water molecules
<b>HA/MgO nanocomposite</b>	
1396.43	Carbonate band
1018.41, 1080.14	v <sub>3</sub> asymmetric stretching of phosphate
555–610	Aluminium bands
3100–3200	Stretching mode of surface hydroxyl Groups and adsorbed water molecules

### TEM analysis

The particle size and morphology of the synthesized HA/Alumina HA/MgO nanocomposite have been examined by TEM. The Figure 3A–3C reveals the TEM images of HA/Alumina and HA/MgO nanocomposite at 250°C. The sample exhibits relatively uniform distribution with nanorod and nanocluster like morphology.<sup>9,13</sup>

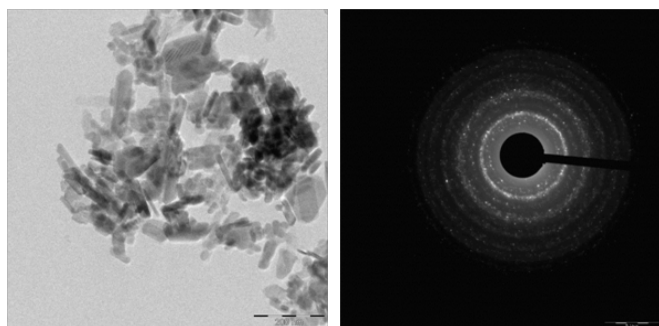


Figure 3A TEM image of HA/Alumina nanocomposite at 250°C.

### UV-visible spectrum analysis

The UV-visible absorption spectra of the samples were recorded in the wavelength range of 200 to 800nm using a Shimadzu UV

1700 UV spectrometer. The band gap energy was calculated by using Einstein formula ( $E=hc/\lambda$ ). Where h is a Planck's constant ( $6.626 \times 10^{-34}$ J), c is the velocity of light ( $3 \times 10^8$ m/s) and  $\lambda$  be the wavelength of the sample recorded (Figure 4A & 4B).

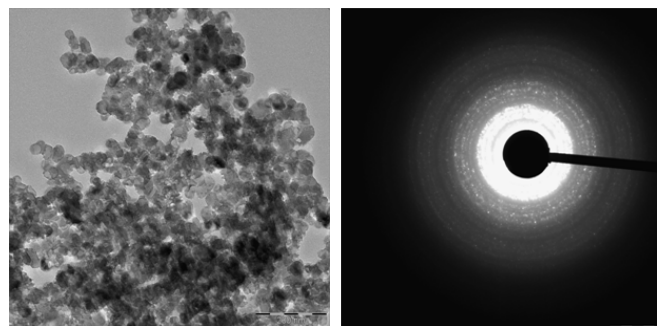


Figure 3B High resolution TEM image at 250°C. 3c) Polycrystalline diffraction pattern of HA/MgO at 250°C recorded.

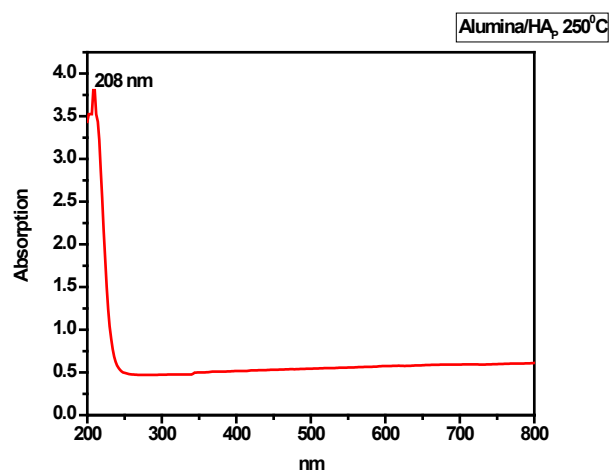


Figure 4A UV-VIS SPECTRUM of HA/Alumina nanocomposite at 250°C.

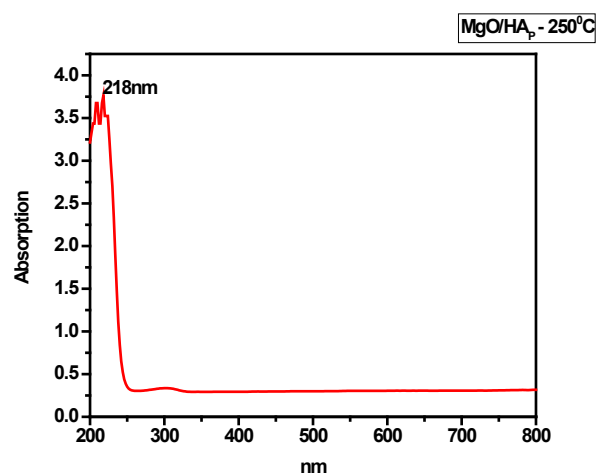


Figure 4B UV-VIS Spectrum of HA/MgO nanocomposite at 250°C.

UV-visible spectroscopy was used to characterize the optical absorption properties of HA/Alumina and HA/MgO nanocomposites at 250°C. We obtained the band gap to be 5.97eV for HA/Alumina at 250°C and MgO/HA at 250°C as 5.689eV respectively.

## Conclusion

In this study, HA/Alumina and HA/MgO nanocomposites were successfully prepared by using the hydrothermal method. The mechanisms of composite formation, crystallite size, crystallinity, morphology, were studied HA/Alumina and HA/MgO nanocomposites. XRD and FTIR investigations showed an intermolecular interaction between HA/Alumina and HA/MgO. The formation of HA<sub>n</sub>/Alumina and HA/MgO nanocomposites confirmed by FTIR, XRD and TEM analysis methods. The formation of HA/Alumina and HA/MgO nanocomposites are polycrystalline in nature. It confirmed in TEM analysis. TEM images further ascertained that HA/Alumina was formed in a short nanorod shape and HA/MgO nanocomposites show nanocluster like morphology. The FTIR measurement shows the appropriate vibrational spectra of HA/Alumina and HA/MgO nanocomposites. The UV-VIS measurements show the band-gap of HA/Alumina and HA/MgO nanocomposites. This study provides a platform for further research on the HA/Alumina and HA/MgO nanocomposites for biomedical applications.

## Acknowledgements

None.

## Conflict of interest

The author declares no conflict of interest.

## References

1. Kirkland NT, Birbilis N, Walker J, et al. *In-vitro* dissolution of magnesium–calcium binary alloys: clarifying the unique role of calcium additions in bioresorbable magnesium implant alloys. *J Biomed Mater Res B Appl Biomater*. 2010;95(1):91–100.
2. Yang Shia, Min Qia, Yao Chenb, et al. MAO–DCPD composite coating on Mg alloy for degradable implant applications. *Materials Letters*. 2011;65(14):2201–2204.
3. Fernandez–Garcia M, Wang X, Belver C, et al. Anatase–TiO<sub>2</sub> Nanomaterials: Morphological/Size Dependence of the Crystallization and Phase Behavior Phenomena. *J Phys Chem C*. 2007;111(2):674–682.
4. Rajkumar M, Meenakshisundaram N, Rajendran V. Development of nanocomposites based on hydroxyapatite/sodium alginate: Synthesis and characterization. *Materials Characterization*. 2011;62(5):469–479.
5. Haque S, Rehman I, Darr JA. Synthesis and characterization of grafted nanohydroxyapatites using functionalized surface agents. *Langmuir*. 2007;23(12):6671–6676.
6. Hu R, Lin CJ, Shi HY. A novel ordered nano hydroxyapatite coating electrochemically deposited on titanium substrate. *J Biomed Mater Res A*. 2007;80(3):687–692.
7. Rajkumar M, Meenakshisundaram N, Rajendran V. *Int J Eng Sci Technol*. 2010;2(6):2437–2444.
8. Rajkumar M, Kavitha K, Prabhu M, et al. Nanohydroxyapatite–chitosan–gelatin polyelectrolyte complex with enhanced mechanical and bioactivity. *Mater Sci Eng C Mater Biol Appl*. 2013;33(6):3237–3244.
9. Milella E, Cosentino F, Licciulli Ai, et al. Preparation and characterisation of titania/hydroxyapatite composite coatings obtained by sol–gel process. *Biomaterials*. 2001;22(11):1425–1431.
10. Varma RS, Saini RK, Dahiya R. *Tetrahedron Lett*. 1997;38:7823.
11. Su–Hee Lee, Hyoun–Ee Kim. *J Am Ceram Soc*. 2007;90(1):50–56.
12. Hae–Won Kim, Long–Hao Li, Young–Hag Koh. Sol–Gel Preparation and Properties of Fluoride–Substituted Hydroxyapatite Powders. *J Am Ceram Soc*. 2004;87(10):1939–1944.
13. Cava S, Tebcherani SM, Souza IA, et al. Structural characterization of phase transition of Al<sub>2</sub>O<sub>3</sub> nanopowders obtained by polymeric precursor method. *Materials Chemistry and Physics*. 2007;103:394–399.